Supporting Information

to

Products of the OH Radical-Initiated Reactions of Furan, 2- and 3-Methylfuran, and 2,3- and 2,5-Dimethylfuran in the Presence of NO

Sara M. Aschmann, Noriko Nishino, Janet Arey* and Roger Atkinson*

Air Pollution Research Center

University of California

Riverside, CA 92521

Pages: 25

Tables: 4

Figures: 12

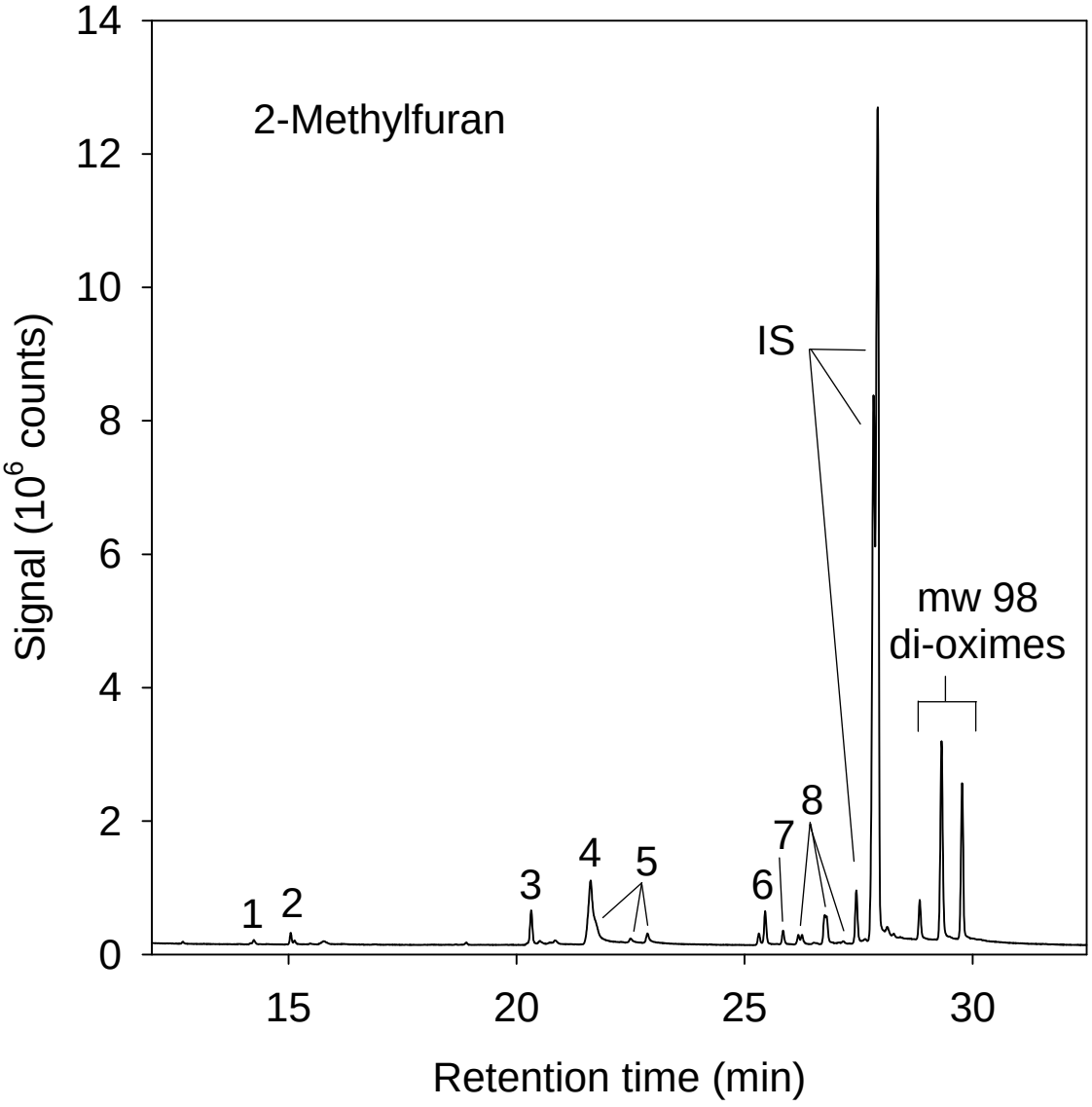

Figure S1. Positive chemical ionization GC-MS total ion chromatogram (TIC) of an extract of a PFBHA-coated denuder sample collected after 2.5 min irradiation of a CH_3ONO – NO – 2-methylfuran – 2,5-hexanedione (internal standard, IS) – air mixture, with 41% consumption of the initially present 2-methylfuran. IS = di-oximes of 2,5-hexanedione, the internal standard; peak #1, mono-oxime of molecular weight (mw) 72 dicarbonyl; peak #2, mono-oxime of $CH_3C(O)CH_2CHO$ (mw 86) formed from OH + 2,5-hexanedione; peaks #3, from derivatizing agent; peak #4, mono-oxime of mw 100 carbonyl; peaks #5, mono-oximes of mw 114 carbonyl; peaks #6, di-oximes of glyoxal; peak #7, di-oxime of methylglyoxal (mw 72); peaks #8, di-oximes of $CH_3C(O)CH_2CHO$ formed from OH + 2,5-hexanedione; and mw 98 di-oximes attributed to $CH_3C(O)CH=CHCHO$.

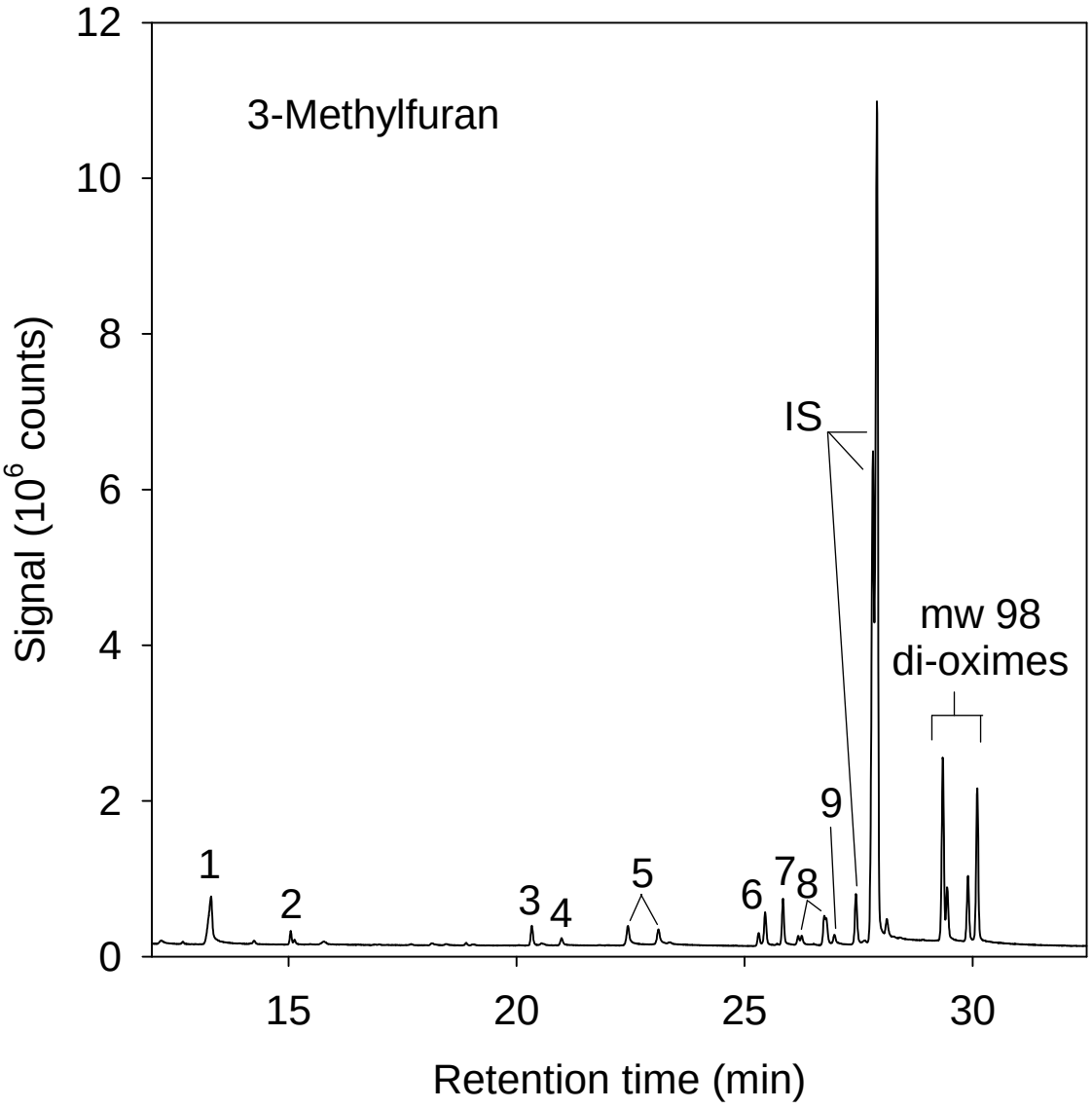

Figure S2. Positive chemical ionization GC-MS total ion chromatogram (TIC) of an extract of a PFBHA-coated denuder sample collected after 4 min irradiation of a CH_3ONO – NO – 3-methylfuran – 2,5-hexanedione (internal standard, IS) – air mixture, with 46% consumption of the initially present 3-methylfuran. IS = di-oximes of 2,5-hexanedione, the internal standard; peak #1, ions at m/z 115 and 97 present; peak #2, mono-oxime of $CH_3C(O)CH_2CHO$ (mw 86) formed from OH + 2,5-hexanedione; peak #3, from derivatizing agent; peak #4, mono-oxime of mw 98 dicarbonyl; peaks #5, mono-oximes of mw 114 carbonyl; peaks #6, di-oximes of glyoxal; peak #7, di-oxime of methylglyoxal (mw 72); peaks #8, di-oximes of $CH_3C(O)CH_2CHO$ formed from OH + 2,5-hexanedione; and mw 98 di-oximes attributed to $HC(O)C(CH_3)=CHCHO$.

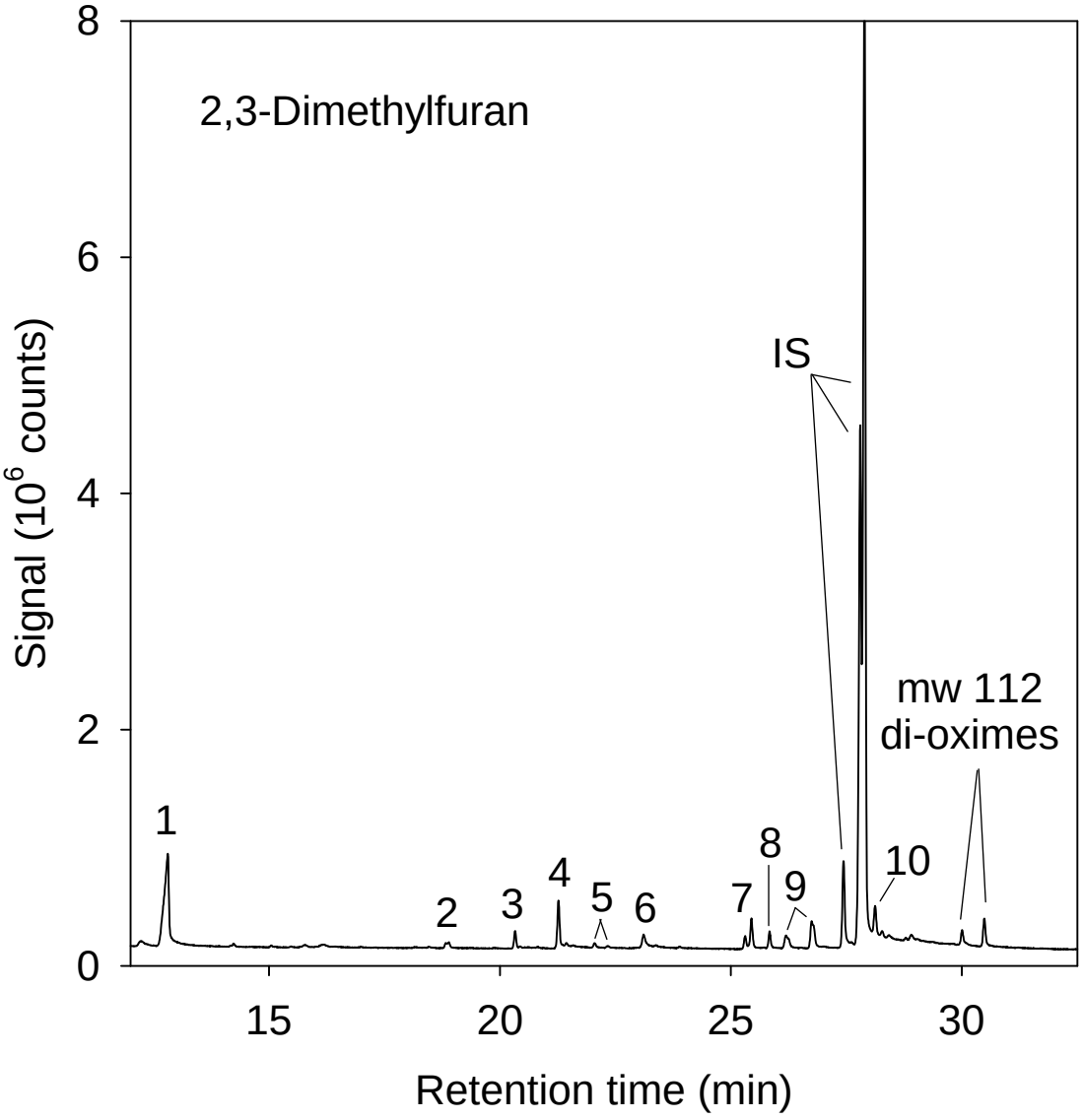

Figure S3. Positive chemical ionization GC-MS total ion chromatogram (TIC) of an extract of a PFBHA-coated denuder sample collected after 2 min irradiation of a CH_3ONO – NO – 2,3-dimethylfuran – 2,5-hexanedione (internal standard, IS) – air mixture, with 49% consumption of the initially present 2,3-dimethylfuran. IS = di-oximes of 2,5-hexanedione, the internal standard; peak #1, mono-oxime of mw 60 carbonyl, with fragment ions at m/z 129 and 111 present; peaks #2 and #3, from derivatizing agent; peak #4, unidentified mono-oxime; peaks #5, mono-oximes of mw 112 dicarbonyl (attributed to $CH_3C(O)C(CH_3)=CHCHO$); peak #6, mono-oxime of mw 114 carbonyl; peaks #7, di-oximes of glyoxal; peak #8, di-oxime of methylglyoxal (mw 72); peaks #9, di-oximes of $CH_3C(O)CH_2CHO$ (mw 86) formed from OH + 2,5-hexanedione, with a contribution to the earliest-eluting of these peaks from biacetyl; peak #10, di-oximes of mw 102 dicarbonyl, with fragment ion indicating loss of H_2O (and hence possibly $CH_3C(O)CH(OH)CHO$ formed as a second-generation product from $CH_3C(O)C(CH_3)=CHCHO$); and mw 112 di-oximes attributed to $CH_3C(O)C(CH_3)=CHCHO$.

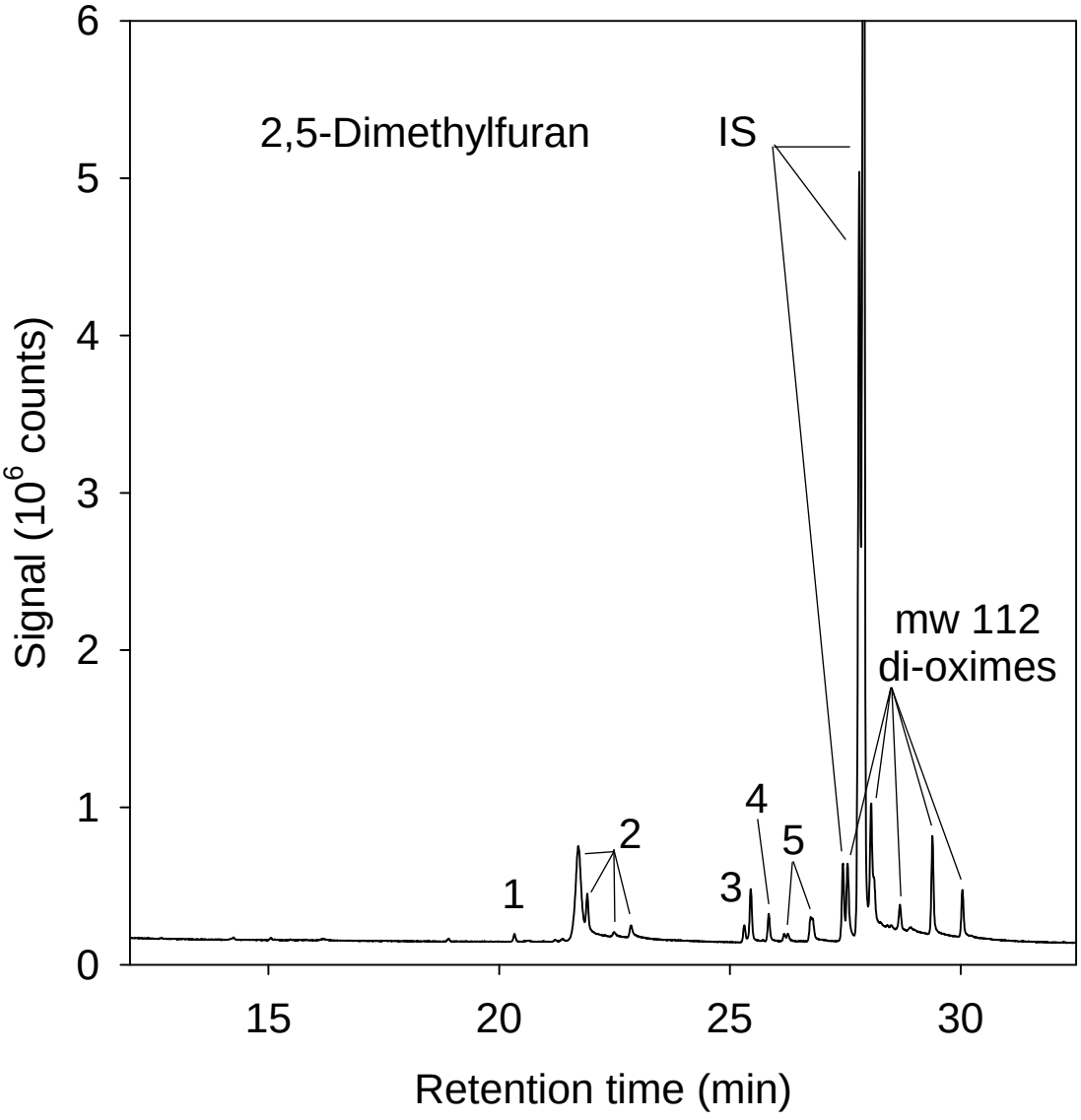

Figure S4. Positive chemical ionization GC-MS total ion chromatogram (TIC) of an extract of a PFBHA-coated denuder sample collected after 1.5 min irradiation of a CH_3ONO – NO – 2,5-dimethylfuran – 2,5-hexanedione (internal standard, IS) – air mixture, with 35% consumption of the initially present 2,5-dimethylfuran. IS = di-oximes of 2,5-hexanedione, the internal standard; peak #1, from derivatizing agent; peaks #2, mono-oximes of mw 114 carbonyl(s); peaks #3, di-oximes of glyoxal; peak #4, di-oxime of methylglyoxal (mw 72); peaks #5, di-oximes of $CH_3C(O)CH_2CHO$ (mw 86) formed from OH + 2,5-hexanedione; and mw 112 di-oximes of $CH_3C(O)CH=CHC(O)CH_3$.

Table S1. Experimental conditions and results for CH_3ONO – NO – furan – 2,5-hexanedione – air irradiations

furan	irradiation time (min)[b]	[furan], ppbV[a]		unsaturated 1,4-dicarbonyl (ppbV)[a,c]
		initial	reacted	
furan	8	1017	582	271, 266
	6	1033	500	257, 261, 255
	4	1029	386	218, 214
	8	1057	622	289, 299, 294, 298, 292
2-methylfuran	3	940.5	464.5	106
	2	895	336	74.3, 74.4
	3	797.5	401.5	86.9, 86.6
	2.5	1016.5	412.5	107, 107
3-methylfuran	3	900.5	506	135, 134
	2	889.5	400.5	115, 115
	2.5	1004	513	144, 142
	2	967	424	126, 129
2,3-dimethylfuran	3	906	583	37.7, 38.6
	2	916	449	30.3, 29.4
	1.5	933.5	354.5	25.4, 25.2
	2	935	459.5	34.0, 33.6
	4[d]	964	592	40.1, 40.9, 39.7
	3[e]	919	449.5	27.0, 26.6
	3[f]	948.5	474	28.9, 27.7
2,5-dimethylfuran	1.5	945	330.5	81.3, 81.1

[a]1 ppbV = 2.40×10^{10} molecule cm^{-3} for the temperature and pressure conditions employed (296 ± 2 K and ~735 Torr pressure).

[b]At a light intensity corresponding to an NO_2 photolysis rate of 0.14 min^{-1}. Unless noted otherwise, PFBHA-coated denuder samples were collected immediately after the irradiation,

with the denuder sampling directly from the chamber and with the denuder inlet protruding into the chamber. 2,5-Hexanedione (225-244 ppbV) was included in the reactant mixture prior to irradiation. The initial CH_3ONO and NO concentrations were ~5 ppmV each.

[c]Measured concentrations of unsaturated 1,4-dicarbonyl [HC(O)CH=CHCHO from furan, $CH_3C(O)CH=CHCHO$ from 2-methylfuran, $HC(O)C(CH_3)=CHCHO$ from 3-methylfuran, $CH_3C(O)C(CH_3)=CHCHO$ from 2,3-dimethylfuran, and $CH_3C(O)CH=CHC(O)CH_3$ from 2,5-dimethylfuran]. In each experiment, the dicarbonyl concentration was determined from the GC-FID peak areas of the di-oxime peaks of 2,5-hexanedione (the internal standard) and of the di- and (if present) mono-oxime peaks of the unsaturated 1,4-dicarbonyl, and the measured concentration of 2,5-hexanedione (from GC-FID analyses of samples collected onto Tenax solid adsorbent; see text), taking into account small differences in the GC-FID response factors for the dicarbonyl di-oximes.[1,2] The entries for a given experiment are from replicate analyses of the extract.

[d]Preliminary experiment carried out with PFBHA-coated denuder samples being collected 156 min after the irradiation period, with the denuder sampling downstream of a cascade impactor. 2,5-Hexanedione (374.5 ppbV) was added after the irradiation.

[e]Preliminary experiment carried out with PFBHA-coated denuder samples being collected 45 min after the irradiation period, with the denuder sampling downstream of a cascade impactor. 2,5-Hexanedione (124 ppbV) was added after the irradiation.

[f]Preliminary experiment carried out with PFBHA-coated denuder samples being collected 1 min after the irradiation period, with the denuder sampling downstream of a cascade impactor. 2,5-Hexanedione (96 ppbV) was included in the reactant mixture prior to irradiation.

Behavior of Unsaturated 1,4-Dicarbonyls during OH + Furan Reactions

For the reaction sequence,

OH + furan $\rightarrow$ α dicarbonyl + other products	(k_{furan})
OH + dicarbonyl $\rightarrow$ products	(k_{OH})
dicarbonyl + $h\nu$ $\rightarrow$ loss of dicarbonyl	(k_{phot})
dicarbonyl $\rightarrow$ wall loss of dicarbonyl	(k_w)

the concentration of the dicarbonyl at time t is given by,

$$[\text{dicarbonyl}]_t = A\,(e^{-x} - e^{-Bx}) \qquad \text{(I)}$$

where $A = \alpha[\text{furan}]_{initial}\{k_{furan}[OH]/(k_{OH}[OH] + k_{phot} + k_w)]\}$, α is the formation yield of dicarbonyl from reaction (1) $B = (k_{OH}[OH] + k_{phot} + k_w)/k_{furan}[OH]$, and x = extent of reaction = $\ln([\text{furan}]_{to}/[\text{furan}]_t)$.[3,4] Hence a fit of Equation (I) to the experimental data leads to values of A and B,[3,4] with the values of B (referred to here and in the manuscript as k_2/k_1) being of particular interest in this study.

Two sets of relevant data were obtained (Table S2); one set from the denuder analyses, with one data point per experiment at a given extent of reaction and with the duration of the experiments being ~1.5 hr, and the second set from continuous irradiations of CH_3ONO – NO – furan – air mixtures with analysis of the unsaturated 1,4-dicarbonyl every ~3 min by direct air sampling atmospheric pressure ionization mass spectrometry (API-MS).[4] In this second set of experiments, the furan (or alkylfuran) concentrations were measured by GC-FID before and after

the irradiations, which were carried out for 21-66 min at a light intensity corresponding to an NO_2 photolysis rate of ~0.035 min^{-1} (a factor of 4 lower than used for the experiments with sample collection onto annular denuders).

Figures S5-S8 show plots of Equation (I) for the experiments with GC analyses of PFBHA-coated denuder samples (i.e., the data presented in Table S1, with each data point in Figures S5-S8 being an average of the replicate unsaturated 1,4-dicarbonyl concentrations for that experiment), together with predictions from Equation (I) with differing values of k_2/k_1 (see also text in the manuscript and the captions to the individual figures). In these denuder experiments, conducted with identical initial CH_3ONO and NO concentrations, for a given furan the OH radical concentrations averaged over the irradiation period were independent of the irradiation time, with ≤13% change in the OH radical concentration for a factor of 2 change in the irradiation time (see the denuder samples in Table S2). Hence the OH radical concentrations could be taken to be constant for the experiments with a given furan in the same Teflon chamber, and for a given furan the relative contributions of photolysis and OH radical reaction were essentially constant for that series of experiments. The data for OH + 2,3-dimethylfuran shown in Figure S8, for two series of experiments in different Teflon chambers with differing OH radical concentrations, are consistent with our assumption that photolysis of 3-methyl-4-oxo-2-pentenal by black lamps was of no importance.

The data from the second set of experiments (those with continuous irradiations and in situ API-MS analyses) are summarized in Table S2 and representative plots of Equation (I) are shown in Figures S9 and S10. In these experiments, with pre- and post-reaction GC-FID analyses of the furan and API-MS analyses of the unsaturated 1,4-dicarbonyl, the OH radical concentrations during the 21-66 min irradiation period were assumed to be constant in order to

calculate the extents of reaction, $\ln([furan]_{to}/[furan]_t)$. While the OH radical concentrations would very likely decrease during the irradiation periods, the effect should have been small because of the low light intensities employed. If the OH radical concentration in an experiment decreased with irradiation time, then the assumption of a constant OH radical concentration would mean that the derived values of k_2/k_1 would be upper limits (see Figure S11).

The data from the two sets of experiments are reasonably consistent (Table S2), with values of k_2/k_1 of ~1.0 for HC(O)CH=CHCHO formation from OH + furan, 0.6-0.9 for formation of $CH_3C(O)CH=CHCHO$ from OH + 2-methylfuran, 0.6-0.8 for formation of $HC(O)C(CH_3)=CHCHO$ from OH + 3-methylfuran, and ~0.5 for formation of $CH_3C(O)C(CH_3)=CHCHO$ from OH + 2,3-dimethylfuran.

Table S2. Experimental conditions and results from analyses of the time-concentration behavior of unsaturated 1,4-dicarbonyls during OH radical-initiated reactions of furans

furan	CH_3ONO (ppmV)	NO (ppmV)	irradiation time (min)[a]	$10^{-7} \times [OH]_{av}$ (molecule cm^{-3})[b]	k_2/k_1	analysis method
furan	2	2	45	1.52	0.8 ± 0.1[c]	API-MS
furan	1	2	66	0.73	1.2 ± 0.1	API-MS
furan	2	1	30	2.81	0.9 ± 0.1	API-MS
furan	5	5	4-8	4.36-4.86	1.03[d]	denuder
2-methylfuran	2	2	33	1.70	0.5 ± 0.1[e]	API-MS
2-methylfuran	1	1	36	1.67	0.6 ± 0.1	API-MS
2-methylfuran	1	2	39	0.93	0.9 ± 0.1	API-MS
2-methylfuran	2	1	21	3.19	0.3 ± 0.1	API-MS
2-methylfuran	5	5	2-3	4.74-5.36	0.90[f]	denuder
3-methylfuran	2	2	27	1.81	0.65 ± 0.1	API-MS
3-methylfuran	1	2	39	0.94	0.55 ± 0.1	API-MS
3-methylfuran	5	5	2-3	5.46-5.71	0.79[g]	denuder
2,3-dimethylfuran	2	2	24	1.60	0.55 ± 0.1	API-MS
2,3-dimethylfuran	1	2	36	0.88	0. 45 ± 0.1	API-MS
2,3-dimethylfuran	5	5	1.5-4	2.96-4.47[h]	0.48[i]	denuder

[a]At light intensities corresponding to NO_2 photolysis rates of 0.14 min^{-1} for experiments with GC-FID analysis of annular denuder samples and ~0.035 min^{-1} for experiments with API-MS analysis.

[b]Calculated from pre- and post-reaction GC-FID analyses of the furans.

[c]See Figure S9.

[d]See Figure S5; four experiments were conducted.

[e]See Figure S10.

[f]See Figure S6; four experiments were conducted.

[g]See Figure S7; four experiments were conducted.

[h]For data denoted by open symbols (○) in Figure S8, the four irradiations were for 1.5-3 min, with calculated OH radical concentrations of (4.21-4.54) × 10^7 molecule cm^{-3}. For the three preliminary experiments (filled symbols (●) in Figure S8), irradiations were for 3-4 min, with calculated OH radical concentrations of (2.96-3.15) × 10^7 molecule cm^{-3}.

[i]See Figure S8.

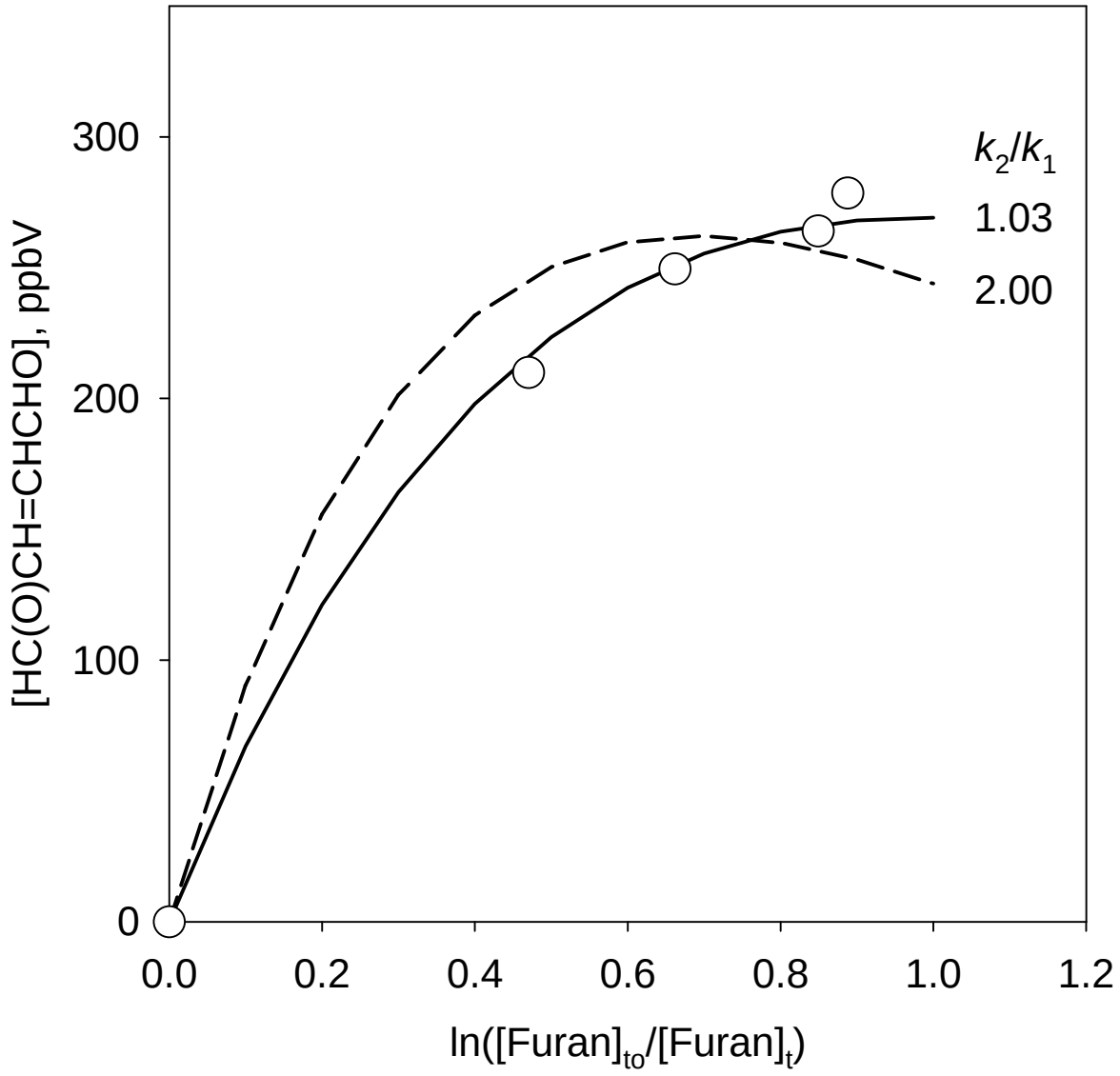

Figure S5. Plot of measured concentrations of HC(O)CH=CHCHO as a function of the extent of reaction, defined as $\ln([\text{furan}]_{to}/[\text{furan}]_t)$, in the OH + furan reactions. Each data point is the average measured concentration from a single experiment (see Table S1). The lines are calculated from the expression [HC(O)CH=CHCHO] = $A\{\exp(-k_1t) - \exp(-k_2t)\}$, where k_1 is the rate of reaction of the furan, k_2 is the rate of reaction of HC(O)CH=CHCHO (by reaction with OH radicals, photolysis and any other loss processes), and A was used as an adjustable constant to match the experimental data in the Y-axis. Note that $\ln([\text{furan}]_{to}/[\text{furan}]_t) = k_1(t - t_o)$ since the OH radical concentration was essentially constant and equal for all four experiments.

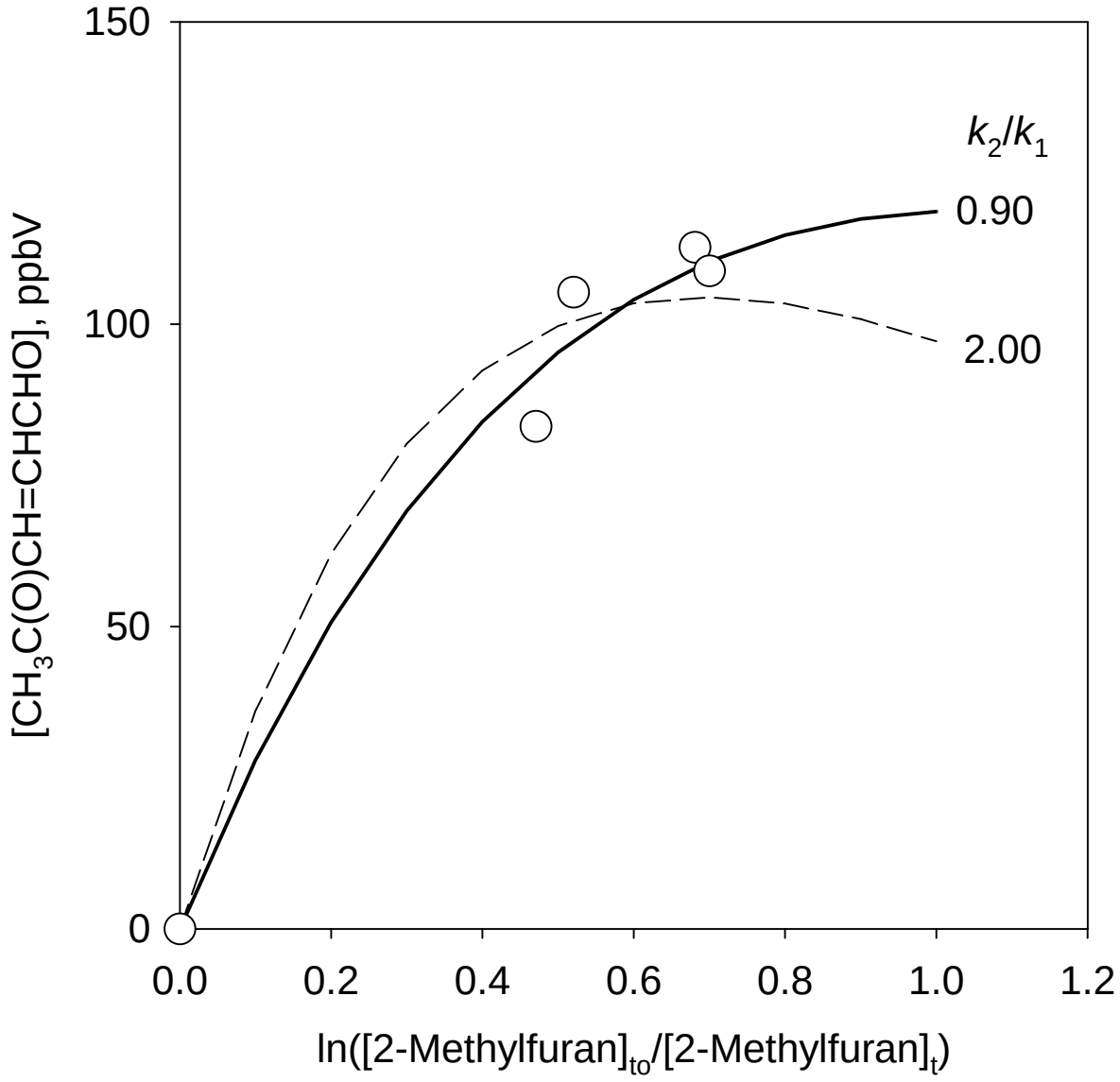

Figure S6. Plot of measured concentrations of $CH_3C(O)CH=CHCHO$ as a function of the extent of reaction, defined as $\ln([2\text{-methylfuran}]_{to}/[2\text{-methylfuran}]_t)$, in the OH + 2-methylfuran reactions. Each data point is the average measured concentration from a single experiment (see Table S1). The lines are calculated from the expression $[CH_3C(O)CH=CHCHO] = A\{\exp(-k_1t) - \exp(-k_2t)\}$, where k_1 is the rate of reaction of the 2-methylfuran, k_2 is the rate of reaction of $CH_3C(O)CH=CHCHO$ (by reaction with OH radicals, photolysis and any other loss processes), and A was used as an adjustable constant to match the experimental data in the Y-axis. Note that $\ln([2\text{-methylfuran}]_{to}/[2\text{-methylfuran}]_t) = k_1(t - t_o)$ since the OH radical concentration was essentially constant and equal for all four experiments.

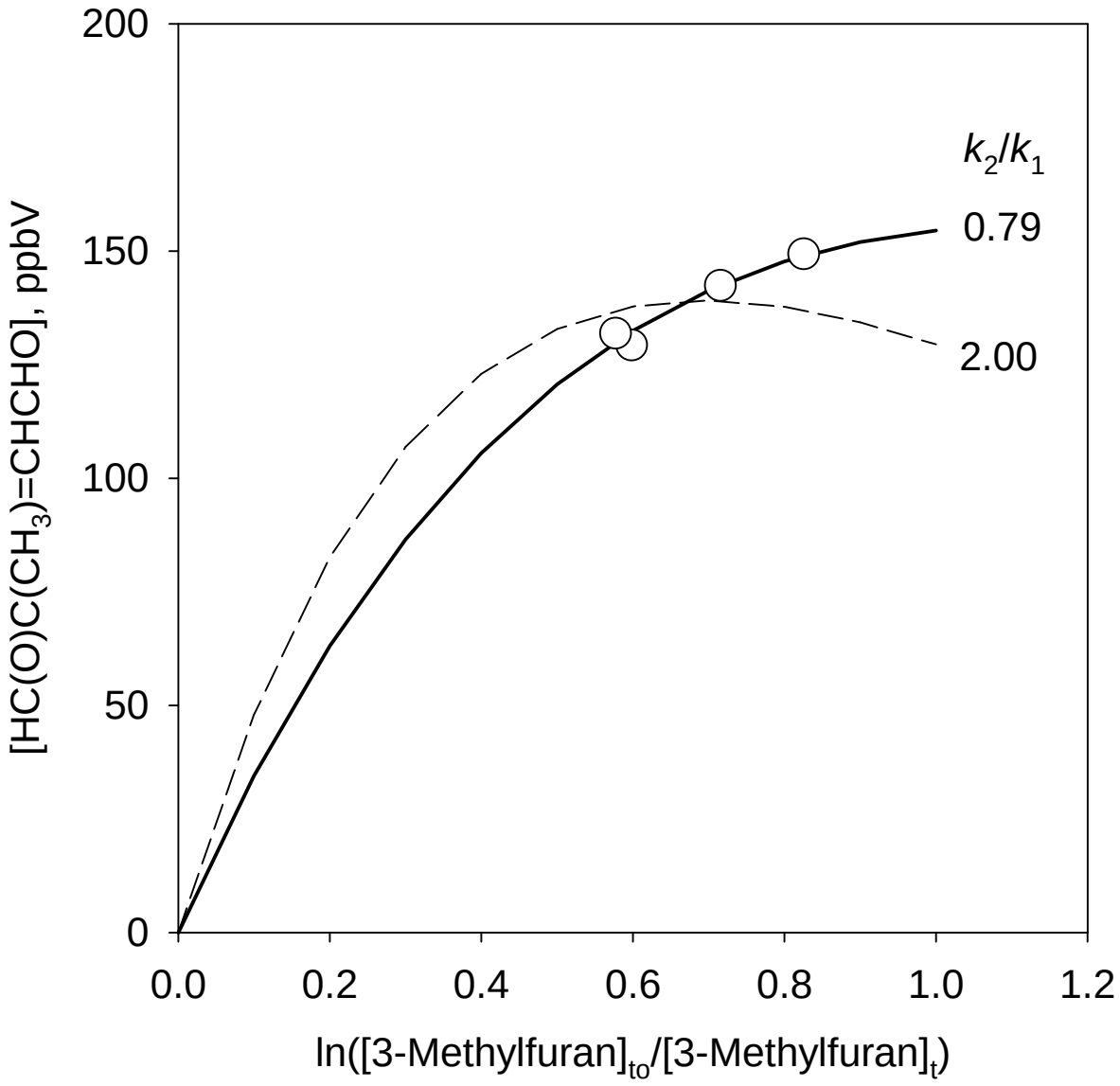

Figure S7. Plot of measured concentrations of $HC(O)C(CH_3)=CHCHO$ as a function of the extent of reaction, defined as $\ln([3\text{-methylfuran}]_{to}/[3\text{-methylfuran}]_t)$, in the OH + 3-methylfuran reactions. Each data point is the average measured concentration from a single experiment (see Table S1). The lines are calculated from the expression $[HC(O)C(CH_3)=CHCHO] = A\{\exp(-k_1t) - \exp(-k_2t)\}$, where k_1 is the rate of reaction of the 3-methylfuran, k_2 is the rate of reaction of $HC(O)C(CH_3)=CHCHO$ (by reaction with OH radicals, photolysis and any other loss processes), and A was used as an adjustable constant to match the experimental data in the Y-axis. Note that $\ln([3\text{-methylfuran}]_{to}/[3\text{-methylfuran}]_t) = k_1(t - t_o)$ since the OH radical concentration was essentially constant and equal for all four experiments.

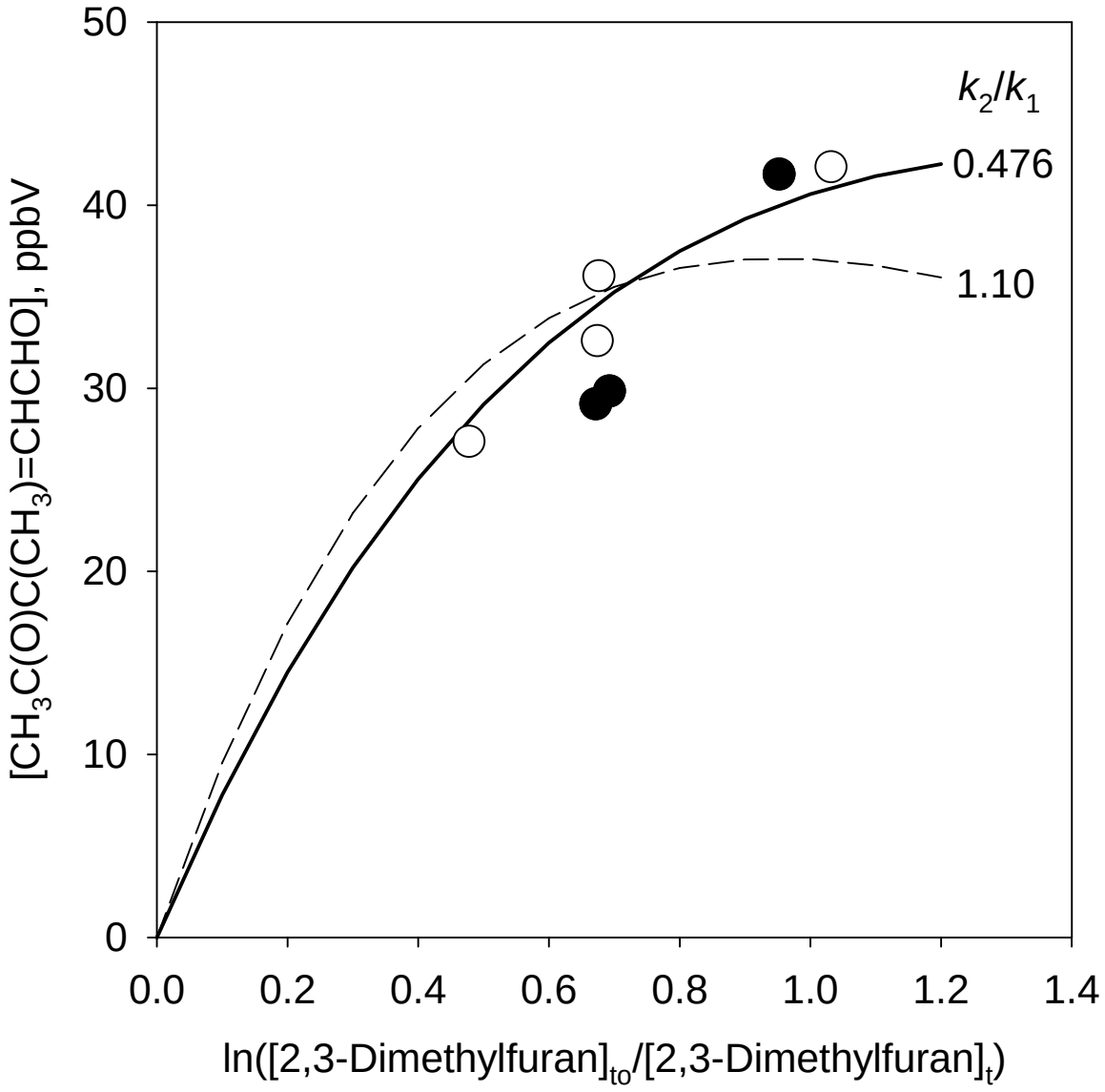

Figure S8. Plot of measured concentrations of $CH_3C(O)C(CH_3)=CHCHO$ as a function of the extent of reaction, defined as $\ln([2,3\text{-dimethylfuran}]_{to}/[2,3\text{-dimethylfuran}]_t)$, in the OH + 2,3-dimethylfuran reactions. Each data point is the average measured concentration from a single experiment (see Table S1). The lines are calculated from the expression $[CH_3C(O)C(CH_3)=CHCHO] = A\{\exp(-k_1t) - \exp(-k_2t)\}$, where k_1 is the rate of reaction of the 2,3-dimethylfuran, k_2 is the rate of reaction of $CH_3C(O)C(CH_3)=CHCHO$ (by reaction with OH radicals, photolysis and any other loss processes), and A was used as an adjustable constant to match the experimental data in the Y-axis. Note that $\ln([2,3\text{-dimethylfuran}]_{to}/[2,3\text{-dimethylfuran}]_t) = k_1(t - t_o)$ since the OH radical concentration was essentially constant and equal for the experiments with the same symbol. ○, experiments with 2,5-hexanedione initially present in the reactant mixtures and with sampling immediately after the irradiation period; ●, preliminary experiments (see Table S1 for conditions and Table S2 for the OH radical concentrations during the experiments).

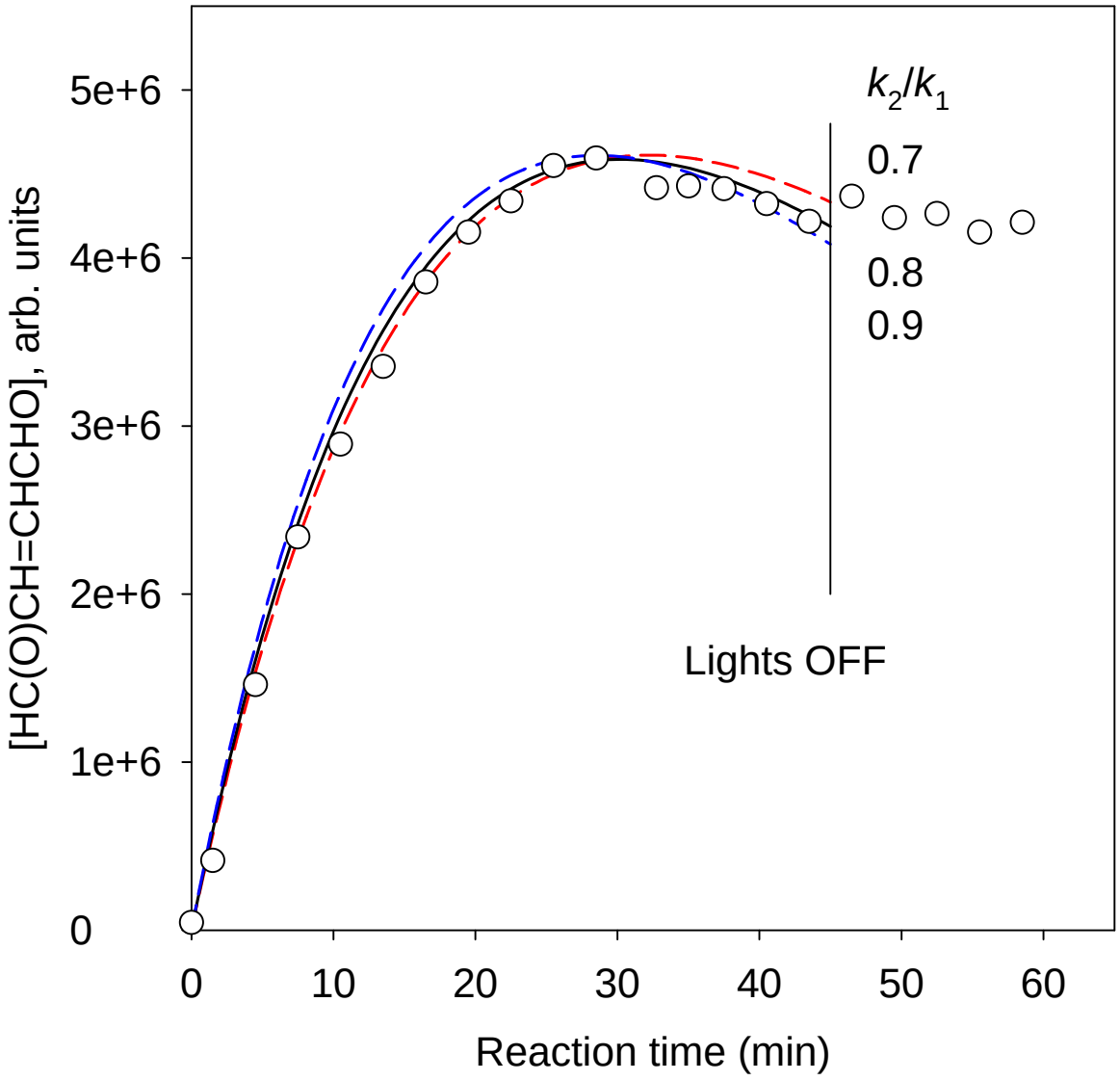

Figure S9. Plot of the API-MS signal attributed to ions of HC(O)CH=CHCHO as a function of the reaction time in an OH + furan reaction (see Table S2 for the experimental conditions). The lights were turned on at 0 min and off at 45 min, and data obtained after the lights were turned off are also shown. The lines are calculated from the expression [HC(O)CH=CHCHO] = $A\{\exp(-k_1 t) - \exp(-k_2 t)\}$, where k_1 is the rate of reaction of the furan, k_2 is the rate of reaction of HC(O)CH=CHCHO (by reaction with OH radicals, photolysis and any other loss processes), and A was used as an adjustable constant to match the experimental data in the Y-axis. A constant OH radical concentration was assumed, with $\ln([\text{furan}]_{to}/[\text{furan}]_t) = k_1(t - t_o)$.

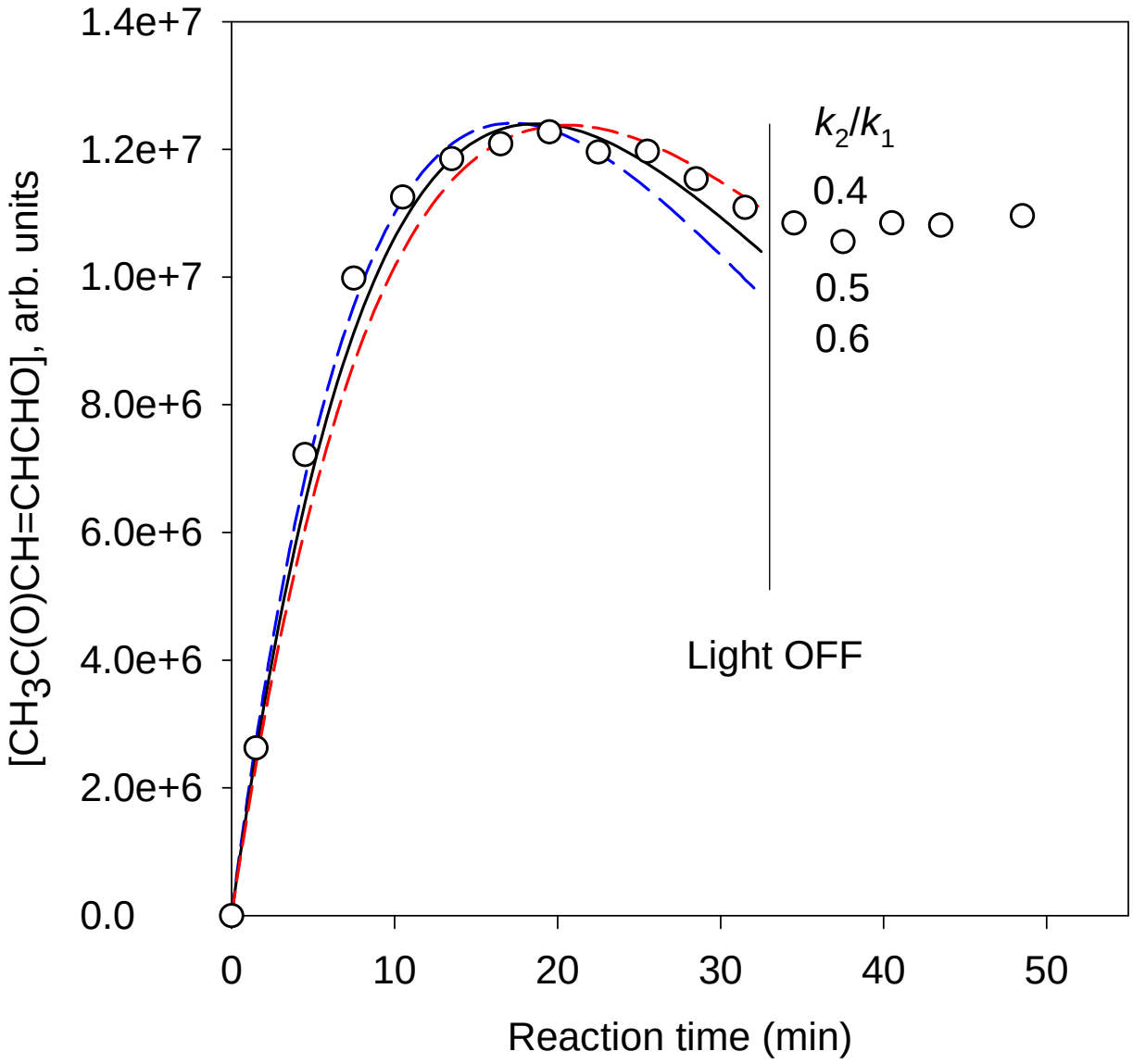

Figure S10. Plot of the API-MS signal attributed to ions of $CH_3C(O)CH=CHCHO$ as a function of the reaction time in an OH + 2-methylfuran reaction (see Table S2 for the experimental conditions). The lights were turned on at 0 min and off at 33 min, and data obtained after the lights were turned off are also shown. The lines are calculated from the expression $[CH_3C(O)CH=CHCHO] = A\{\exp(-k_1t) - \exp(-k_2t)\}$, where k_1 is the rate of reaction of the 2-methylfuran, k_2 is the rate of reaction of $CH_3C(O)CH=CHCHO$ (by reaction with OH radicals, photolysis and any other loss processes), and A was used as an adjustable constant to match the experimental data in the Y-axis. A constant OH radical concentration was assumed, with $\ln([2\text{-methylfuran}]_{to}/[2\text{-methylfuran}]_t) = k_1(t - t_o)$.

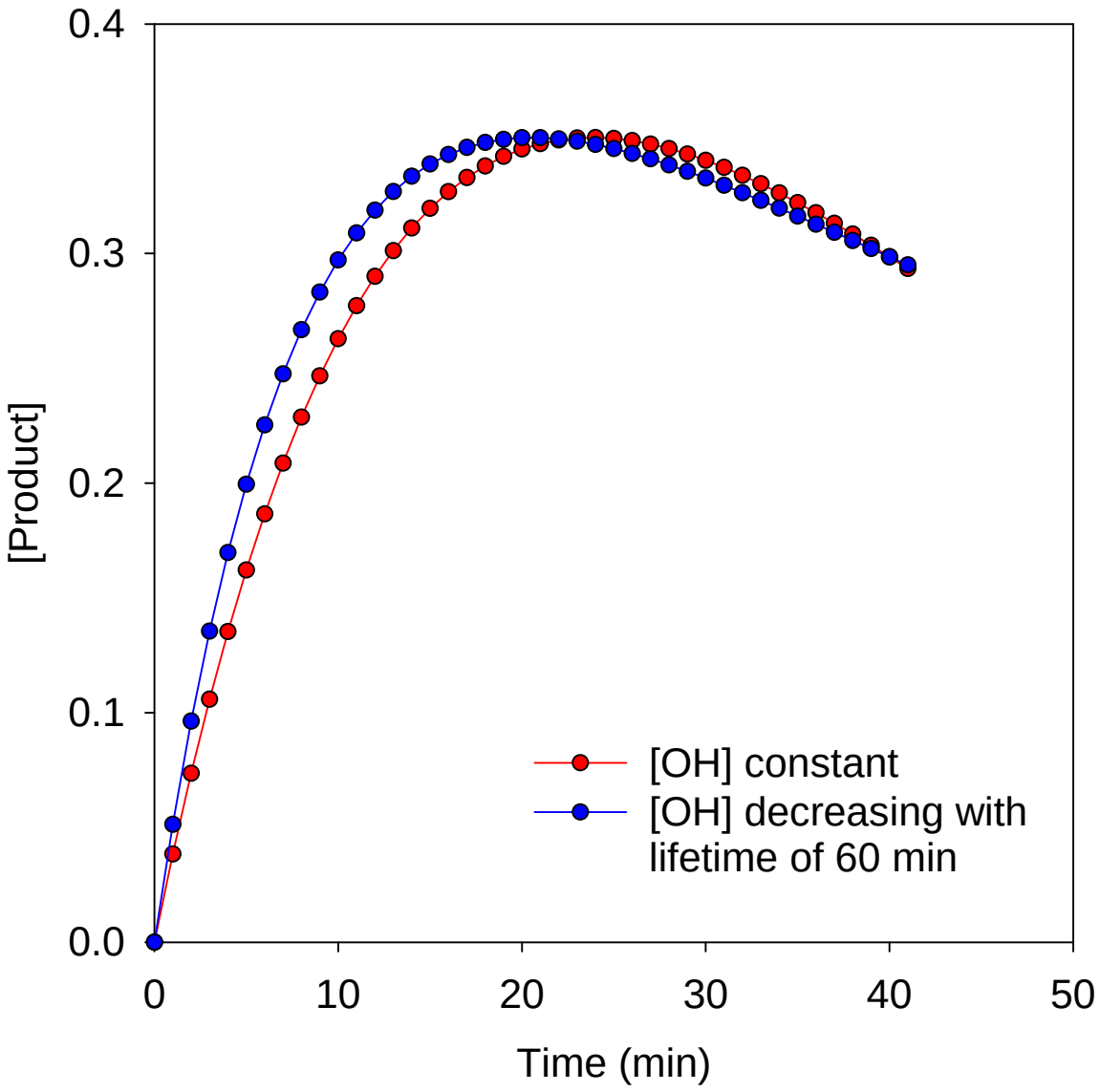

Figure S11. Plots of Equation (I), with (red) a constant OH radical concentration for 40 min, and (blue) an OH radical concentration which decayed exponentially with a lifetime of 60 min (approximately corresponding to that expected for the light intensity employed in the experiments with in situ API-MS detection of the unsaturated 1,4-dicarbonyls). The integrated OH radical concentration at t = 40 min was identical in both calculations. The maximum [Product] occurs earlier in the simulation with decreasing OH radical concentration, which would be interpreted as a higher value of k_2/k_1 if an constant OH radical concentration was assumed to derive the extents of reaction, x, in Equation (I).

Formation of unsaturated 1,4-dicarbonyls from OH + aromatic hydrocarbons

Unsaturated 1,4-dicarbonyls and 1,2-dicarbonyls are also formed from the OH radical-initiated reactions of monocyclic aromatic hydrocarbons.[2,5-10] Glyoxal, methylglyoxal and 2,3-butanedione formation yields from the toluene, *o*-, *m*- and *p*-xylene, and 1,2,3-, 1,2,4- and 1,3,5-trimethylbenzene reactions have been obtained at low NO_2 concentrations.[2,7,11] The 3-hexene-2,5-dione formation yields of Bethel et al.[7] from the OH + *p*-xylene and OH + 1,2,4-trimethylbenzene reactions are identical within the experimental uncertainties with the co-product glyoxal[2,12] and methylglyoxal[2] formation yields, respectively. The 3-hexene-2,5-dione formation yields can then be used to place the unsaturated 1,4-dicarbonyl relative yield data of Arey et al.[9] onto an absolute basis (assuming that all of the unsaturated 1,4-dicarbonyls have the same collection and derivatization efficiency and that the GC-MS total ion chromatogram signal responses are the same). The resulting comparison of the 1,2-dicarbonyl[2,7,11] and unsaturated 1,4-dicarbonyl[9] formation yields are shown in Figure S12 and Table S3. While the formation yields of 1,4-butenedial are similar to those of its presumed co-products (Table S4), the formation yields of 4-oxo-2-pentenal, 2-methyl-1,4-butenedial and 3-methyl-4-oxo-2-pentenal are significantly lower than those of their assumed co-products (Table S4).

Table S3. Molar formation yields (%) of 1,2-dicarbonyls and of their unsaturated 1,4-dicarbonyl presumed co-products at atmospheric pressure of air and low NO_2 concentrations

aromatic	1,2-dicarbonyl[a]	presumed co-product[b]
toluene	$(CHO)_2$, 26.0 ± 2.2	$CH_3C(O)CH=CHCHO$, 7.7 $HC(O)C(CH_3)=CHCHO$, 1.2
	$CH_3C(O)CHO$, 21.5 ± 2.9	$HC(O)CH=CHCHO$, 24.1
o-xylene	$(CHO)_2$, 12.7 ± 1.9	$CH_3C(O)C(CH_3)=CHCHO$, 0.6 $HC(O)C(CH_3)=C(CH_3)CHO$, not observed
	$CH_3C(O)CHO$, 33.1 ± 6.1	$CH_3C(O)CH=CHCHO$, 14.4
	$CH_3C(O)C(O)CH_3$, 18.5[c]	$HC(O)CH=CHCHO$, 16.3
m-xylene	$(CHO)_2$, 11.4 ± 0.7	$CH_3C(O)CH=C(CH_3)CHO$, 1.6
	$CH_3C(O)CHO$, 51.5 ± 8.5	$CH_3C(O)CH=CHCHO$, 25.4 $HC(O)C(CH_3)=CHCHO$, 11.5
p-xylene	$(CHO)_2$, 38.9 ± 4.7	$CH_3C(O)CH=CHC(O)CH_3$, 40.5 (32.3[d])
	$CH_3C(O)CHO$, 18.7 ± 2.2	$HC(O)C(CH_3)=CHCHO$, 4.4
1,2,3-TMB	$(CHO)_2$, 4.7 ± 2.4	$CH_3C(O)C(CH_3)=C(CH_3)CHO$, 0.1
	$CH_3C(O)CHO$, 15.1 ± 3.3	$CH_3C(O)C(CH_3)=CHCHO$, 3.2
	$CH_3C(O)C(O)CH_3$, 52.0[d]	$CH_3C(O)CH=CHCHO$, 16
1,2,4-TMB	$(CHO)_2$, 8.7 ± 1.6	$CH_3C(O)C(CH_3)=CHC(O)CH_3$, 3.0
	$CH_3C(O)CHO$, 27.2 ± 8.1	$CH_3C(O)C(CH_3)=CHCHO$, 0.2 $CH_3C(O)CH=CH(CH_3)CHO$, 0.4 $CH_3C(O)CH=CHC(O)CH_3$, 25.6 (30.9[d]) $HC(O)C(CH_3)=C(CH_3CHO$, not observed
	$CH_3C(O)C(O)CH_3$, 10.2	$HC(O)C(CH_3)=CHCHO$, 2.4
1,3,5-TMB	$CH_3C(O)CHO$, 58.1 ± 5.3	$CH_3C(O)CH=C(CH_3)CHO$, 7.2

[a]From Nishino et al.,[2] unless noted otherwise, at low NO_2 concentration.
[b]From Arey et al.,[9] using the formation yields of 3-hexene-2,5-dione from the *p*-xylene and 1,2,4-trimethylbenzene reactions measured by Bethel et al.[7] to place the relative yield data of Arey et al.[9] on an absolute basis.
[c]From Atkinson and Aschmann.[11]
[d]From Bethel et al.[7]

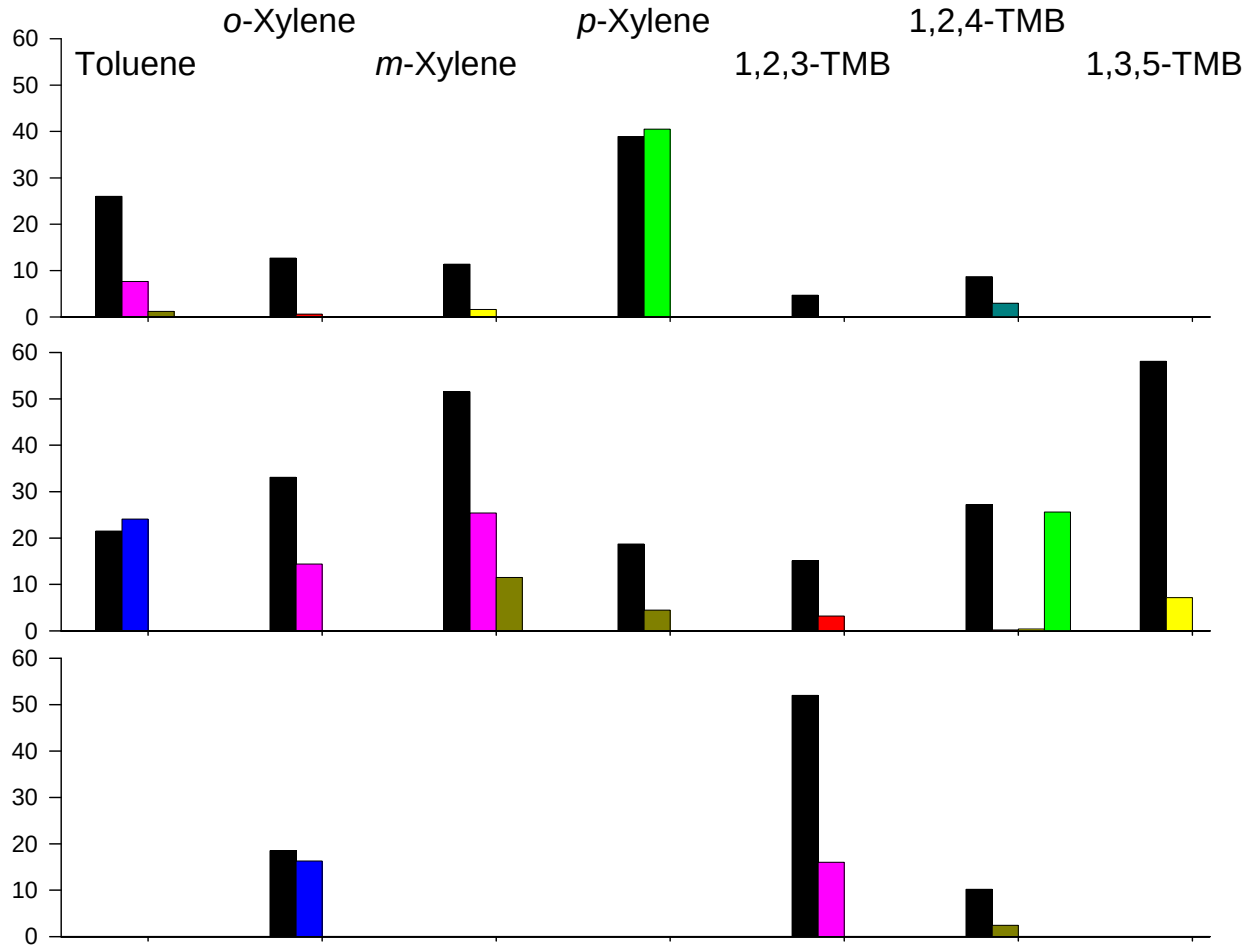

Figure S12. Top panel: glyoxal and co-product unsaturated 1,4-dicarbonyl formation yields from the aromatics. Middle panel: methylglyoxal and co-product unsaturated 1,4-dicarbonyl formation yields. Bottom panel: 2,3-butanedione and co-product unsaturated 1,4-dicarbonyl formation yields. The data are from Table S3. Black bars refer to the 1,2-dicarbonyls, blue to HC(O)CH=CHCHO, pink to $CH_3C(O)CH=CHCHO$, tan to $HC(O)C(CH_3)=CHCHO$, red to $CH_3C(O)C(CH_3)=CHCHO$, bright yellow to $CH_3C(O)CH=C(CH_3)CHO$, green to $CH_3C(O)CH=CHC(O)CH_3$, and turquoise to $CH_3C(O)C(CH_3)=CHC(O)CH_3$.

Table S4. Ratios of (molar yield of unsaturated 1,4-dicarbonyl)/(molar yield of 1,2-dicarbonyl co-product) calculated using the data presented in Table S3 for OH + methyl-substituted benzenes

unsaturated 1,4-dicarbonyl	from reaction of OH radicals with					
	toluene	*o*-xylene	*m*-xylene	*p*-xylene	123-TMB	124-TMB
HC(O)CH=CHCHO	1.12	0.88				
$CH_3C(O)CH=CHCHO$	≥0.31[a]	0.44	≥0.64[a]		0.31	
$HC(O)C(CH_3)=CHCHO$	≥0.07[a]		≥0.44[a]	0.24		0.24
$CH_3C(O)C(CH_3)=CHCHO$		≥0.05[a]			0.21	

[a]Taking into account the measured formation yield of the other unsaturated 1,4-dicarbonyl (see Table S3), which may be a lower limit. For example, for OH + *m*-xylene, the co-products to methylglyoxal (51.5% measured yield) are $CH_3C(O)CH=CHCHO$ (25.4% measured yield) and $HC(O)C(CH_3)=CHCHO$ (11.5% measured yield). The ratio ($CH_3C(O)CH=CHCHO$ yield)/(methylglyoxal yield) = 25.4/(51.5-11.5) = 0.64. Since the measured $HC(O)C(CH_3)=CHCHO$ formation yield may be a lower limit, the ratio ($CH_3C(O)CH=CHCHO$ yield)/(methylglyoxal yield) ≥0.64.

References

1. Scanlon, J. T.; Willis, D. E. Calculation of Flame Ionization Detector Relative Response Factors using the Effective Carbon Number Concept. *J. Chromat. Sci*. **1985**, *23*, 333-340.
2. Nishino, N.; Arey, J.; Atkinson, R. Formation Yields of Glyoxal and Methylglyoxal from the Gas-Phase OH Radical-Initiated Reactions of Toluene, Xylenes, and Trimethylbenzenes as a Function of NO_2 Concentration. *J. Phys. Chem. A* **2010**, *114*, 10140-10147.
3. Baker, J.; Arey, J.; Atkinson, R. Rate Constants for the Gas-Phase Reactions of OH Radicals with a Series of Hydroxyaldehydes at 296 ± 2 K. *J. Phys. Chem. A* **2004**, *108*, 7032-7037.
4. Nishino, N.; Arey, J.; Atkinson, R. Formation and Reactions of 2-Formylcinnamaldehyde in the OH Radical-Initiated Reaction of Naphthalene. *Environ. Sci. Technol.* **2009**, *43*, 1349-1353.
5. Smith, D. F.; McIver, C. D.; Kleindienst, T. E. Primary Product Distribution from the Reaction of Hydroxyl Radicals with Toluene at ppb NO_x Mixing Ratios. *J. Atmos. Chem.* **1998**, *30*, 209-228.
6. Smith, D. F.; Kleindienst, T. E.; McIver, C. D. Primary Product Distributions from the Reaction of OH with *m*-, *p*-Xylene, 1,2,4- and 1,3,5-Trimethylbenzene. *J. Atmos. Chem.* **1999**, *34*, 339-364.
7. Bethel, H. L.; Atkinson, R.; Arey, J. Products of the Gas-Phase Reactions of OH Radicals with *p*-Xylene and 1,2,3- and 1,2,4-Trimethylbenzene: Effect of NO_2 Concentration. *J. Phys. Chem. A* **2000**, *104*, 8922-8929.

8. Gómez Alvarez, E.; Viidanoja, J.; Muñoz, A.; Wirtz, K.; Hjorth, J. Experimental Confirmation of the Dicarbonyl Route in the Photo-Oxidation of Toluene and Benzene. *Environ. Sci. Technol.* **2007**, *41*, 8362-8369.

9. Arey, J.; Obermeyer, G.; Aschmann, S. M.; Chattopadhyay, S.; Cusick, R. D.; Atkinson, R. Dicarbonyl Products of the OH Radical-Initiated Reaction of a Series of Aromatic Hydrocarbons. *Environ. Sci. Technol*. **2009**, *43*, 683-689.

10. Aschmann, S. M.; Arey, J.; Atkinson, R. Rate Constants for the Reactions of OH Radicals with 1,2,4,5-Tetramethylbenzene, Pentamethylbenzene, 2,4,5-Trimethylbenzaldehyde, 2,4,5-Trimethylphenol, and 3-Methyl-3-hexene-2,5-dione and Products of OH + 1,2,4,5-Tetramethylbenzene. *J. Phys. Chem. A* **2013**, *117*, 2556-2568.

11. Atkinson, R.; Aschmann, S. M. Products of the Gas-Phase Reactions of Aromatic Hydrocarbons: Effect of NO_2 Concentration. *Int. J. Chem. Kinet.* **1994**, *26*, 929-944.

12. Volkamer, R.; Spietz, P.; Burrows, J.; Platt, U. High-Resolution Absorption Cross-Section of Glyoxal in the UV-Vis and IR Spectral Ranges. *J. Photochem. Photobiol. A: Chem.* **2005**, *172*, 35-46.